Optical clocks based on molecular vibrations as probes of variation of the proton-to-electron mass ratio

David Hanneke, Boran Kuzhan and Annika Lunstad

Physics & Astronomy Department, Amherst College, Amherst, Massachusetts 01002, USA

E-mail: `dhanneke@amherst.edu`

Abstract. Some new physics models of quantum gravity or dark matter predict drifts or oscillations of the fundamental constants. A relatively simple model relates molecular vibrations to the proton-to-electron mass ratio μ. Many vibrational transitions are at optical frequencies with prospects for use as highly accurate optical clocks. We give a brief summary of new physics models that lead to changes in μ and the current limits on drifts and oscillation amplitudes. After an overview of laboratory procedures, we give examples of molecules with experiments currently in development or underway. These experiments' projected systematic and statistical uncertainties make them leading candidates in next-generation searches for time-variation of μ.

1. Introduction

Atoms and molecules are compact, naturally occurring systems that can be isolated from their environment in relatively small numbers. Many pairs of quantum states within an atom or a molecule have transition energies corresponding to light in radio through optical frequencies that are conveniently produced in a laboratory. Atomic and molecular transitions are the most accurate frequency references in existence [1]. A microwave atomic transition defines the SI second. Optical transitions will serve as next-generation time and frequency standards [2]. Because of their high accuracy, atomic and molecular transitions are sensitive probes of physics typically associated with energy scales much higher than the transition energy itself. They serve to demonstrate and test known physics, such as parity violation and quantum electrodynamics, as well as to search for new physics, such as time-reversal violation, quantum gravity, and dark matter [3].

Some new physics models predict changes to the values of fundamental constants, which are typically referred to in terms of dimensionless values such as the fine structure constant $\alpha = e^2/(4\pi\epsilon_0\hbar c)$ or the proton-to-electron mass ratio $\mu = m_p/m_e$. These changes could take the form of slow drifts or steady oscillations. In this manuscript, we focus on the use of molecules to search for variation in the proton-to-electron mass ratio. Unlike atoms, molecules have direct sensitivity to changes in μ. Their vibrational and rotational degrees of freedom involve the motion of the inertial masses of the nuclei, and the strength and length of their chemical bonds involve the electron mass.

The mass ratio μ is sensitive to a variety of new effects because the proton and electron acquire their masses by different mechanisms. Protons, neutrons, and their combinations in atomic nuclei are bound states of quarks and gluons. Around $99\,\%$ of their mass arises from the strong interaction. Each mass is proportional to the quantum chromodynamics energy scale Λ_{QCD}, ignoring the small contribution from the quark masses [4]. This common proportionality is why we talk about molecular vibration and rotation as being sensitive to the proton mass when the literal sensitivity is to the reduced mass of the nuclei. By contrast, the electron is a fundamental particle. Its mass arises from its interaction with the Higgs field. Thus, μ is sensitive to new physics that couples to gluons, quarks, electrons, or the Higgs.

2. Changing constants

2.1. Models

Many theories of new physics beyond the Standard Model give rise to dynamical "constants". These theories often postulate new scalar fields or extra spatial dimensions. Couplings to standard particles will cause our (3+1)-dimensional constants to change with the dynamics of the new fields or the expanding or contracting length scales of the new dimensions. Several models are reviewed in [4]. In many of these models, a common underlying mechanism causes correlations in the values of the fundamental constants as they change. For example, some models predict fractional changes in Λ_{QCD} (and thus m_p and μ) to be around 40 times larger than changes in α. Many models link the constants to cosmological evolution and thus predict drifts over long timescales. They typically involve new massless fields.

By contrast, new massive fields can induce oscillations in the fundamental constants [5, 6, 7]. Bosonic matter that is lightweight enough that the particle wavepackets overlap forms a coherent classical wave. The field ϕ oscillates at the Compton frequency $f_\phi = m_\phi c^2/h$, where m_ϕ is the mass of the new particle. The oscillation amplitude ϕ_0 is related to the field's energy density ρ_ϕ through

$$\phi_0 = \sqrt{\frac{\hbar^3}{c^5}} \frac{\sqrt{2\rho_\phi}}{m_\phi}. \tag{1}$$

(Here, we write the field amplitude with units of mass, as in [5]; see [7, App. A] for different conventions.) Since it is massive, this field could potentially make up a

significant fraction of the galaxy's dark matter; if it does, then this energy density is $\rho_{\text{DM}} \approx 0.4$ GeV/cm^3 [8]. New couplings to Standard-Model particles would transfer oscillations in the dark matter field amplitude to effective oscillations in the fundamental constants. In a generic model, the new couplings to each Standard-Model particle are independent, but the fundamental constants would oscillate with a common frequency and phase. In some specific models, such as the relaxion model [9, 10], the couplings to Standard-Model particles are related to each other as well. In these cases, there is a model-specific relation between the oscillation amplitudes of the various fundamental constants. The allowed dark matter particle masses span many orders of magnitude, from $m_\phi \sim 10^{-21}$ eV/c^2 (the de Broglie wavelength should fit in the halo of the smallest dwarf galaxies) to 10^{-1} eV/c^2 (the density of particles in the local dark matter should be sufficient to form a classical field) [6, 11]. This mass range corresponds to oscillation frequencies in the range $f_\phi \sim 10^{-7}$–10^{13} Hz.

2.2. Current Limits

The tightest constraints on these models come from direct searches for drifts of atomic and molecular spectral lines as well as indirect limits on oscillations from equivalence-principle tests. Observations of molecular spectra in high-redshift astrophysical scenarios constrain

$$|\Delta\mu|/\mu < 10^{-6} - 10^{-7} \quad \text{over} \quad \sim 10^{10} \text{ yr.} \tag{2}$$

Comparisons with present-day spectra have been made for a variety of species, including NH_3, CS, and H_2CO [12], CH_3OH [13], H_2 [14], and CO [15].

The tightest constraint on present-day drift comes from comparison of an Yb$^+$ optical clock with a Cs microwave clock [16], which set the limit

$$\dot{\mu}/\mu = (-0.8 \pm 3.6) \times 10^{-17} \text{ yr}^{-1}. \tag{3}$$

This limit is an improvement by a factor of approximately two over other recent results comparing Yb and Sr optical clocks against Cs [17, 18]. In each of these cases, the optical transition is electronic in nature and has almost no sensitivity to changes in μ. The hyperfine microwave transition's μ-dependence is in the cesium nuclear magnetic dipole moment. The relationship of this moment to μ is model-dependent [19].

Optical clocks have surpassed microwave clocks in accuracy [2]. For this reason, next-generation experiments are focusing on comparing two optical transitions. Molecules possess optical transitions with sensitivity to μ because their vibrational and rotational degrees of freedom involve the motion of the nuclei themselves. Molecular clocks are not yet at the accuracy of atomic clocks, though many molecular species have the potential to rival atomic clocks in terms of their ultimate systematic effects. The current best limit on μ-drift that uses a molecule is based on two vibrational states in different electronic potentials in KRb. The limit set is [20]

$$\dot{\mu}/\mu = (-0.30 \pm 1.0) \times 10^{-14} \text{ yr}^{-1}. \tag{4}$$

Earlier experiments used an optical transition in a beam of SF_6 to set a six-times less stringent limit [21].

We are unaware of any experimental results that directly probe for oscillations in μ. We can estimate limits on μ oscillation amplitudes from indirect probes by assuming a phenomenological model of the dark-matter coupling. Fundamental constants that change in time would appear to violate the equivalence principle; prior experiments searching for equivalence-principle violations provide constraints on the dark matter coupling coefficients [5, 7]. These constraints tend to be m_ϕ-independent up to some threshold mass. For example, torsion balance experiments [22] restrict the coupling parameter $|d_g| < 7.2 \times 10^{-6}$ for masses whose Compton wavelength is greater than the Earth's radius ($m_\phi < 3 \times 10^{-14}$ eV/c^2). Here, d_g is a dimensionless parameter characterizing the strength of a linear coupling of ϕ to the gluon field; a value of one would represent a force of the same strength as gravity. At higher masses, the restriction relaxes to approximately $|d_g| < 3 \times 10^{-2}$. See [5] for a discussion and more detailed exclusion plots; see [7] for a discussion of a phenomenological model with quadratic coupling ϕ^2. If we assume the only coupling is to the gluon field, the oscillation amplitude of the fractional change in μ is given by [5, 7]

$$\frac{\Delta\mu}{\mu} = d_g \phi_0 \sqrt{\frac{4\pi G}{\hbar c}} = \frac{d_g \sqrt{\rho_\phi}}{m_\phi} \frac{\hbar \sqrt{8\pi G}}{c^3}. \tag{5}$$

Here, G is Newton's gravitational constant. Assuming further that the new field's energy density is equal to the local dark matter density, the equivalence principle limits correspond to an oscillation amplitude of approximately

$$\frac{|\Delta\mu|}{\mu} < \begin{cases} 5 \times 10^{-36} \text{ eV}/(m_\phi c^2), & m_\phi < 3 \times 10^{-14} \text{ eV}/c^2 \\ 2 \times 10^{-32} \text{ eV}/(m_\phi c^2), & m_\phi > 3 \times 10^{-14} \text{ eV}/c^2 \end{cases}. \tag{6}$$

In terms of the dark matter's Compton frequency, which shows up as the experimental modulation frequency, these limits correspond to

$$\frac{|\Delta\mu|}{\mu} < \begin{cases} 1 \times 10^{-21} \text{ Hz}/f_\phi, & f_\phi < 7 \text{ Hz} \\ 5 \times 10^{-18} \text{ Hz}/f_\phi, & f_\phi > 7 \text{ Hz} \end{cases}. \tag{7}$$

For example, at an oscillation frequency of 1 mHz ($m_\phi = 4 \times 10^{-18}$ eV/c^2), μ is already constrained to oscillate with an amplitude below $\sim 10^{-18}$. At 1 kHz ($m_\phi = 4 \times 10^{-12}$ eV/c^2), the constraint is $\sim 5 \times 10^{-21}$. Since the oscillation amplitude scales as m_ϕ^{-1}, the low-mass/low-frequency end of the range is the place where molecular clocks have the greatest chance to improve over equivalence-principle limits.

There exist models where the dark matter can become bound to the Earth or Sun such that it would have substantially larger densities than the galactic average [23]. The ensuing larger oscillation amplitudes would be most pronounced if m_ϕ is within a few orders of magnitude of 10^{-10} eV/c^2 ($f_\phi = 10^4$ Hz) for dark matter bound to the Earth and 10^{-15} eV/c^2 (10^{-1} Hz) if bound to the Sun. In these scenarios, the higher-than-galactic-average dark matter densities would make it easier for molecular experiments to reach the limits set by equivalence-principle tests.

3. Gaining sensitivity to constants

3.1. Sensitivity in general

A search for time-variation in μ begins by choosing two quantum states that depend differently on the mass ratio. For a single state, we can write an absolute sensitivity factor q_μ that quantifies the absolute energy shift ΔE for a fractional change in μ:

$$\Delta E = q_\mu \frac{\Delta \mu}{\mu}. \tag{8}$$

An experiment requires two states with different sensitivity factors. One then monitors the transition frequency

$$hf = E' - E'' \tag{9}$$

looking for changes

$$h\,\Delta f = \Delta E' - \Delta E'' = (q'_\mu - q''_\mu)\frac{\Delta \mu}{\mu}. \tag{10}$$

For present-day searches, we often want as large a frequency shift as possible. To compare the absolute shift of various transitions, we define the absolute sensitivity of a transition:

$$f_\mu \equiv \mu \frac{\partial f}{\partial \mu} = \frac{q'_\mu - q''_\mu}{h}, \tag{11}$$

such that

$$\frac{\Delta \mu}{\mu} = \frac{\Delta f}{f_\mu}. \tag{12}$$

The quantity f_μ gives the absolute frequency shift of the transition for a fractional shift in μ. For example, if $f_\mu = 100$ THz, then a shift in μ at 10^{-16} would give a 10 mHz shift in the transition frequency.

In the literature, one often encounters the relative sensitivity factor K_μ

$$\frac{\Delta \mu}{\mu} = \frac{1}{K_\mu}\frac{\Delta f}{f}, \tag{13}$$

which is sometimes called the relative enhancement factor. It is related to the absolute sensitivity by $K_\mu = f_\mu/f$. The relative sensitivity is useful in contexts where the precision with which one can measure a frequency shift scales with the frequency. An example is the Doppler-broadened lines common in astrophysical data. In a laboratory context, relative sensitivity can be useful in cases of accidental degeneracies of levels with different absolute sensitivities. In these cases, it might be possible to achieve high precision in $\Delta\mu/\mu$ despite a relatively lower-precision laboratory frequency measurement. For example, a measurements done with transition frequency f in the microwave could have absolute sensitivity f_μ several orders of magnitude larger, in the optical range. The experimental enhancement comes only if one can directly measure the frequency difference between the two states. Appropriate near-degeneracies have been identified in Cs_2 [24] and O_2^+ [25], and used for a $\dot{\mu}$ measurement in KRb [20].

In applying these sensitivity factors to oscillating constants, the molecular and dark-matter coherence times need to be considered. The dark matter is expected to be moving at the galactic virial speed $v \sim 10^{-3}c$ [26], which would lead to oscillation quality factors of order $Q \sim 10^6$ and coherence times $\tau_{\rm coh} \sim 10^6/f_\phi$ [27, 5, 28]. The duration of a single measurement T_m should be shorter than $\tau_{\rm coh}$ so that the signal does not average to zero. If the total duration τ of multiple measurements is also less than $\tau_{\rm coh}$, then the dark matter's phase coherence can be used to maintain sensitivity to μ variation [5, 28, 29]. The sensitivity is suppressed for measurement durations longer than $\tau_{\rm coh}$ or experiments where the dark matter phase is allowed to vary randomly for each individual measurement [28, 30, 29].

3.2. Sensitivity in molecules

The scaling of molecular energies with μ is well-known and has long been used to explain the spectra of isotopologues [31, III.2.g]. A low-order expansion of diatomic molecular energy with vibrational quantum number v and total angular momentum J is

$$E/(hc) = T_e + \omega_e(v + \tfrac{1}{2}) - \omega_e x_e(v + \tfrac{1}{2})^2 + B_e J(J+1), \qquad (14)$$

where the expansion coefficients are given in the traditional units of wavenumbers. The electronic energy T_e is independent of μ. The vibrational coefficient ω_e scales as $1/\sqrt{\mu}$ (that is, $d\omega_e/\omega_e = -\tfrac{1}{2}\, d\mu/\mu$). The lowest anharmonicity coefficient $\omega_e x_e$ and the rotational constant B_e each scale as $1/\mu$. The scaling of coefficients in higher-order expansions may be found in [31, 32, 33, 34]. Given these scalings, the absolute sensitivity of this molecular state is

$$q_\mu = hc \left[-\tfrac{1}{2}\omega_e(v + \tfrac{1}{2}) + \omega_e x_e(v + \tfrac{1}{2})^2 - B_e J(J+1) \right]. \qquad (15)$$

Vibrational transitions hold the potential for the highest sensitivity. The vibrational coefficient is typically much larger than the rotational coefficient, and angular momentum conservation prevents transitions with large ΔJ. For small v, q_μ increases linearly with v; vibrational transitions within the harmonic part of the potential have relative sensitivity $K_\mu = -\tfrac{1}{2}$. Higher in the potential, the anharmonic term reduces the absolute sensitivity, causing it to head back toward zero near dissociation. This reduction makes sense, as near dissociation the system has properties closer to two atoms than a molecule. The maximum sensitivity occurs for vibrational states of energy approximately 3/4 of the dissociation energy [35, 24]. Figure 1 shows the sensitivity of vibrational states in the O_2^+ molecule, and clearly shows the initial linear growth with v and maximum at $v = 28$.

Although this manuscript focuses on variation in μ, some transitions may also have sensitivity to variation in the fine structure constant α. This is especially true of any transition involving states with different spin–orbit couplings or different relativistic corrections to their electronic potentials [36, 37].
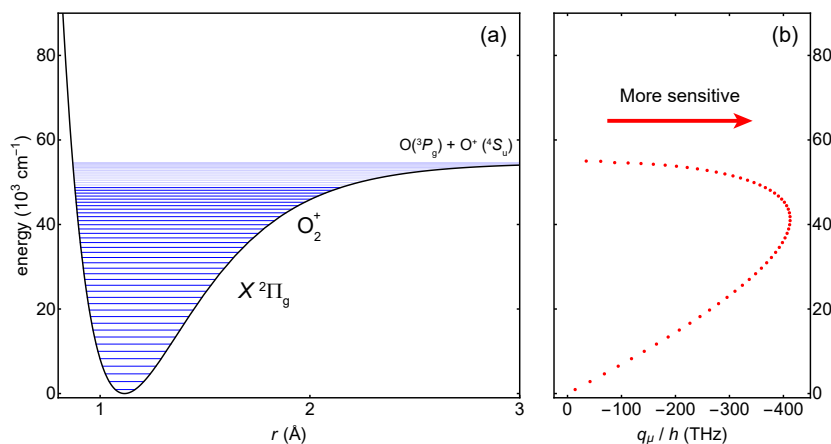
Figure 1. Vibrational levels and absolute sensitivity for the O_2^+ ground $^2\Pi_g$ state. (a) Potential curve. Horizontal lines indicate the energies of vibrational states. Dark lines indicate levels that have been observed experimentally [38]. Light lines fill in the calculated energies of the remaining levels [39]. (b) Absolute sensitivity of each vibrational state. The values are negative because larger μ would reduce the vibrational energies.

4. Experiments with molecules

4.1. Probing the transition, state preparation, and measurement

Most experimental proposals focus on narrow-line vibrational transitions with high absolute sensitivity f_μ. Narrow lines afford longer coherent probe times, and thus faster averaging of statistical uncertainties (section 5.2). In many – but not all – cases, a nonpolar molecule is chosen so the vibrational transitions within an electronic state are electric-dipole ($E1$) forbidden. They can still be driven as electric quadrupole ($E2$) or two-photon transitions. In these precision measurements, a thorough analysis of systematic effects (section 5.1) also plays an important role. Long probe times are facilitated by trapping the molecules. Ion traps and optical lattices can provide tight confinement that eliminates first-order Doppler shifts. Experiments searching for a drifting μ probe the relevant transition frequencies multiple times over the course of a year or more and fit a line with slope $\dot{f}$.

To get a sense for how an experiment searching for oscillations in μ might proceed, we can look to recent work using atoms to search for oscillations in α. For oscillations with a period longer than the experiment cycle-time, one can record the result of each experiment and Fourier transform the data [5, 28, 40]. For periods shorter than a single experiment, a dynamical decoupling pulse sequence can enhance the sensitivity to AC modulation of the molecular frequency [41, 30, 42, 40]. The particular pulse sequence chosen shapes a frequency filter function [29] and would have to be modified during a search through the wide frequency space. If care is taken to synchronize subsequent dynamical decoupling sequences to the oscillations, the signal can maintain its sensitivity

to μ up to $\tau \sim \tau_{\mathrm{coh}}$. If the μ-oscillation phase is allowed to vary for each measurement, the signal has only quadratic sensitivity to the oscillation amplitude [30, 29].

Alternatively, experiments using traditional spectroscopy techniques [43] such as polarization spectroscopy will show direct AC modulation of their signal [44, 45]. For example, the signal might be a photodiode's current that corresponds to the transmission though a molecular vapor cell of a certain frequency and polarization of light. Such techniques often rely on steady-state behavior that is only present on timescales much longer than the molecular state spontaneous emission time. For times much shorter than $1/\gamma$ (γ being the natural linewidth in non-angular frequency units), non-steady-state behavior impedes the signal from tracking the molecular frequency. Thus, high-frequency modulations of μ are suppressed in the measured frequency shifts. This measured shift needs to be corrected as [44]

$$\frac{\Delta\mu}{\mu} = \frac{1}{K_\mu}\left(\frac{\Delta f}{f}\right)_{\mathrm{actual}} = \frac{1}{K_\mu}\left(\frac{\Delta f}{f}\right)_{\mathrm{measured}}\sqrt{1 + \left(\frac{f_\phi}{\gamma}\right)^2}. \tag{16}$$

A variety of choices exist for state preparation and measurement. Some state-preparation procedures create the molecule from other resources. Bi-alkali molecules may be prepared by photoassociating them from ultracold atoms [35, 20]. Molecular ions can be photoionized from the corresponding neutral molecule [46]. Other procedures prepare the state through dissipation. Molecules with near-closed transitions are amenable to optical pumping [47]. Molecular ions co-trapped with atomic ions can use a quantum projection protocol [48].

State-detection procedures can be classified by whether they destroy the molecule or not. State-selective photodissociation can be followed by photofragment imaging [49], by mass analysis in an ion trap or time-of-flight mass spectrometer, or simply by observing molecule loss [50]. Another destructive technique is state-selective chemistry, such as laser-induced charge transfer with a background gas [46]. Optical cycling with fluorescence detection [47] provides non-destructive detection for molecules with diagonal Franck-Condon factors. Quantum-logic spectroscopy [51, 48] is a general-purpose technique for detecting the state of a molecular ion by transferring it to a co-trapped atomic ion that is amenable to fluorescence detection.

A single molecular transition is not sufficient to detect a change in μ. It must be compared to another reference that has different absolute sensitivity and comparable measurement accuracy. For searches for μ drifts, optical atomic clocks [2] provide a suitable reference. They are usually based on electronic transitions that are sensitive to α variation, but have little sensitivity to μ variation. Separate experiments searching for α variation [16, 3] can help attribute any observed change to the molecular transition or the atomic reference. An optical frequency comb can readily compare light at different wavelengths. Alternatively, the same molecule often has many transitions with different f_μ, and two or more transitions could be monitored for differential drifts. Such self-reference could lead to common systematic effects that may improve the ultimate accuracy achieved.

When searching for oscillations in μ, the laser itself may be able to serve as the reference. In optical clock experiments [2], the short-term stability of the laser comes from referencing it to an optical resonance of a two-mirror Fabry-Pérot interferometer. The optical resonance frequency is set by the distance between the two mirrors, which is maintained by a rigid spacer such as ultra-low-expansion glass or crystalline silicon. The spacer's length has very little sensitivity to μ. For frequencies below the lowest mechanical resonance (typically of order 10 kHz), the length is sensitive to changes in the Bohr radius and thus in α and the electron mass [52, 44, 42, 40]. (While the electron mass has dimensions, the sensitivity is to mass changes relative to the average mass; this ratio is dimensionless [45].) Dedicated experiments [52, 44, 42, 40] searching for oscillation in α and m_e can help attribute any observed oscillations to changes in μ, α, or m_e. For even lower frequencies, the spacer's length is subject to thermal drifts and other perturbations.

4.2. Example molecules

Most experiments to date have focused on searches for long-term drifts and oscillation periods longer than a single experiment cycle. To give a sense of the variety of approaches underway, we list a sample of molecules with active experimental work.

KRb: The current best drift limit using molecules comes from photoassociated KRb [20]. The experiment exploits an accidental near-degeneracy between the ground $X\,^1\Sigma^+$ state and the overlapping, shallow $a\,^3\Sigma^+$ potential to achieve absolute sensitivities in the terahertz with a microwave experiment ($f_\mu = 9.45(4)$ THz, $K_\mu = 14\,890(60)$). This experiment yielded the statistics-limited result: $\dot{\mu}/\mu = (-0.30\pm1.00_{\text{stat}}\pm0.16_{\text{syst}})\times 10^{-14}$ yr^{-1}. As a heteronuclear molecule, its primary systematic effect is blackbody radiation, which will require additional calculations and calibrations to reach higher accuracy.

Sr$_2$: Two-photon Raman transitions in lattice-confined photoassociated Sr$_2$ can have sensitivities of up to $f_\mu \approx -7.5$ THz [35]. Because of the photoassociation process, the natural choice for such a transition is between a vibrational state near the dissociation limit and one deeper in the potential. These molecules have a $X\,0_g^+$ ground electronic state and no hyperfine structure, so experiments using the $J = 0$ rotational state should be largely insensitive to magnetic-field systematic effects. Raman clock transitions have been driven coherently in molecules confined to a 1D optical lattice [49]. Importantly, the lattice and two-photon lasers were all chosen in a manner to suppress any differential light/AC-Stark shifts of the clock states. Residual light shifts from imperfect control of the Raman beam intensities remain the leading systematic effect.

N$_2^+$: This ion has been produced in its rovibrational ground state by resonance-enhanced multi-photon ionization (REMPI) and co-trapped with Ca$^+$ atomic ions [46]. The lowest vibrational transition ($v = 0 \rightarrow 1$, $f_\mu = -32$ THz) in its $X\,^2\Sigma_g^+$ electronic ground state has been driven as an electric-quadrupole transition [53]. The molecule's lowest excited electronic state ($A\,^2\Pi_u$) provides a convenient electric-dipole transition.

For example, the excited state's $v' = 2$ level can be accessed with a laser of wavelength ~ 787 nm. It has been used to apply a state-dependent optical dipole force and detect the population in the X state's ground rovibrational state by use of a quantum-nondemolition technique [54].

O_2^+: Proposals to use this ion include driving two-photon transitions from the ground vibrational state to states with sensitivities as high as $f_\mu = -398$ THz ($v' = 28$ or 29) [39] or driving electric-quadrupole transitions as high as $v' = 6$ ($f_\mu = -151$ THz) [55] or even higher [56]. The most common isotope of oxygen (^{16}O, 99.8 % abundance) has no nuclear spin, and thus the molecule has no hyperfine structure. In our own lab, we have photoionized a supersonically expanded molecular beam of O_2 to produce O_2^+ in its ground vibrational state.

H_2^+, HD^+: Several experiments exist with high-precision spectroscopy of these simplest of molecules [50, 57]. Since it is possible to calculate the theory with high accuracy, a main goal of experiments with molecular hydrogen ions is to determine values of fundamental constants, including μ itself [58, 59]. They are also viable candidates for measuring μ-variation [60, 61].

TeH^+: This polar molecule's relatively deep potential allows for high-sensitivity dipole-allowed vibrational transitions. For example, $v = 0 \leftrightarrow v' = 8$ has $f_\mu = -170$ THz [62]. It has near perfect overlap of vibrational wavefunctions (diagonal Franck-Condon factors) in its ground $X_1 0^+$ and excited $X_2 1$, a_2, and $b 0^+$ states. This feature should allow optical pumping for state preparation and quasi-cycling for state detection, with potential reduction in experiment dead time and corresponding improvement in statistical uncertainty [47].

5. Long-term prospects

There are slightly more than two orders of magnitude between the best limit on μ drifts set with molecules and those set with atoms. Many molecules show prospects for closing this gap and going beyond. Several of the above molecules are estimated to be able to achieve systematic and statistical uncertainties comparable to or better than current optical atomic clocks. They should be able to reach fractional frequency instabilities at $< 10^{-18}$. Fractional limits at this level should be comparable to or better than equivalence-principle limits for μ modulation by the lightest dark matter particles. Limits at higher modulation frequencies from heavier particles are much more stringent and will be more challenging to match.

5.1. Systematic uncertainties

Molecular clocks are subject to many of the same systematic effects as atomic clocks. These effects are reviewed in [2]. There are several important differences to consider with the extra vibrational and rotational structure of molecules. For example, many of the proposed experiments use two vibrational levels in the same electronic state,

such that some systematic effects may be common. The energy difference of adjacent vibrational and rotational states are relatively smaller than electronic states, which can alter the scale of some effects.

Electric-field (Stark) shifts have the largest potential to show this changed magnitude. Eigenstates of an unperturbed molecule do not have electric dipole moments, so Stark shifts are second-order effects. From second-order perturbation theory, they are therefore inversely proportional to the energy difference of states of opposite parity. Since rotational energies are much smaller than typical atomic energies, these shifts can be larger in molecules. For molecules with internal electronic angular momentum, even small electric fields can quickly become nonperturbative and can polarize the molecule [63]. This effect arises because there are two projections of this angular momentum on the internuclear axis. The projections combine to form parity eigenstates that are nearly degenerate. These so-called Λ- or Ω-doublets are split only due to a Coriolis coupling with the overall rotation of the molecule.

In order to suppress these potentially large Stark shifts, several experiments use homonuclear molecules. In such molecules, nuclear exchange symmetry forces all rotational states to have the same parity, which eliminates half the rotational states and makes the molecule nonpolar. Since the closest states of opposite parity are excited electronic states, the Stark shifts are suppressed. Thus, homonuclear molecules should have relatively small sensitivity to stray electric fields, to the oscillating electric fields of ion traps, and to blackbody radiation. Nonetheless, AC Stark shifts from applied laser radiation are still expected to be a major source of systematic uncertainties [49, 39, 55]. For experiments in an optical lattice, it will be important to tune the lattice laser wavelength such that there is no differential AC Stark shift between the two clock states [35, 49]. For polar molecules, the Stark shifts are in general not small. There are some cases, however, where the scalar polarizability cancels, leaving only the tensor polarizability. In these cases, it should be possible to null Stark shifts by averaging over multiple transitions with different M and M' quantum numbers [62].

Magnetic field (Zeeman) shifts appear with any molecular magnetic dipole moment. States with electronic angular momentum often have magnetic dipole moments of order a Bohr magneton μ_B and shifts of order $\mu_B/h = 1.4 \times 10^{10}$ Hz/T. These shifts can be suppressed by around 10^3 if the spin and orbital magnetic moments cancel ($\Lambda = -2\Sigma$), such as in the states ${}^2\Pi_{1/2}$ and ${}^3\Delta_1$. Magnetic dipoles from the molecule's rotation and nuclear spins are typically smaller than μ_B by of order 10^3 because of the heavier nuclear mass [64]. Linear Zeeman shifts can be nulled in a transition by driving $M = 0 \leftrightarrow M' = 0$ or (when such states do not exist) by calculating the average of $M \leftrightarrow M'$ and $-M \leftrightarrow -M'$. Second-order Zeeman shifts can arise from mixing with other states. After calibrating the field-dependence of this shift, it can be calculated by measuring the value of the magnetic field with a first-order-shifted transition.

Doppler shifts arise from relative motion of the molecule and laser source. First-order Doppler shifts are suppressed by tight confinement in a trap, which also facilitates long probe times. Residual first-order shifts, such as relative motion within an

apparatus, can be monitored by probing the molecules from different directions. Second order Doppler shifts – a relativistic time dilation effect – arise from nonzero mean-squared speed, such as from finite temperature or micromotion in an ion trap. This is the largest systematic uncertainty in ion-based atomic clocks (at 6×10^{-19}, [65]) and is expected to be a limiting uncertainty in ion-based molecular clocks as well.

Among other shifts, the quadrupolar electric field in ion traps will interact with molecular states that have an electric quadrupole moment. States with $J = 0$ or $\frac{1}{2}$ have no such moment, so the shift is exactly zero. Collisional/density shifts could play a role at high densities in 1D optical lattices. General relativity causes a gravitational redshift of 10^{-18} at 1 cm height differences. This will be important if the reference clock is not at the same location (and height) as the molecule. Implementation-specific shifts will arise as well. While the largest systematic effect will depend on the particular molecule and experiment, several estimates have shown the potential for uncertainties on the shifts to be of order 10^{-18} [66, 61, 56, 39, 62], comparable to those of optical atomic clocks.

5.2. Statistical uncertainties

Statistical uncertainties are limited by the number and duration of experiments. An order-of-magnitude estimate of the statistical uncertainty δf of a frequency measurement is given by [2]

$$\delta f \sim \frac{1}{\sqrt{N T_m \tau}}, \tag{17}$$

where N is the number of molecules probed, T_m is the duration of a single measurement, and τ is the total measurement duration. The precise uncertainty will depend on technical details, such as the pulse sequence employed. Equation (17) assumes negligible time is dedicated to state preparation, measurement, and pulse durations in any Ramsey sequence. It further assumes that the statistical uncertainty is limited by quantum projection noise [67]. For transitions with extremely narrow natural linewidths, such as vibrational overtones of nonpolar molecules, the probe time T_m will be limited by technical considerations like the laser linewidth. For polar molecules, it may be limited by the transition's natural linewidth.

Given this frequency uncertainty, the fractional uncertainty in μ is

$$\frac{\delta \mu}{\mu} = \frac{\delta f}{f_\mu} = \frac{\delta f}{K_\mu f}. \tag{18}$$

As an example, consider a vibrational transition with $K_\mu = -0.5$ probed by a laser of wavelength 1 μm ($f = 300$ THz) for a duration of $T_m = 1$ s. It would achieve a statistical uncertainty $\delta \mu / \mu \sim 7 \times 10^{-15} / \sqrt{N(\tau/\text{s})}$, which would average down to the present limit of 3.6×10^{-17} in around ten hours with one molecule. As discussed in section 4.1, the molecular measurement must be referenced to another transition with different absolute μ sensitivity and similar accuracy. This example assumes an atomic reference with no sensitivity to μ and the same frequency accuracy $\delta f / f$.

For probes of oscillating constants by use of dynamical decoupling, the statistical uncertainty in (17) is still the correct order of magnitude [30]. In a such a multi-pulse sequence, other technical considerations may come into play. For example, the pulse fidelity may limit the number of pulses and thus the duration of an individual experiment T_m. As the search frequency increases, the finite pulse duration will need to be included in the filter-function design. The overall scaling will change if either T_m or τ approach the dark matter coherence time τ_{coh} [28, 30, 29].

Searches for oscillations by use of traditional spectroscopy techniques [43] will have statistical limits based on quantities such as shot noise in a photodetector. For a given signal S and noise δS, one can achieve a fractional frequency uncertainty of [2]

$$\delta f = \frac{\delta S}{dS/df}. \tag{19}$$

Here, dS/df is a discriminator that says how much the signal changes for a given frequency shift. This slope is typically steeper for narrower resonances, such that we can approximate the statistical uncertainty by

$$\delta f \sim \frac{\delta S}{S/\gamma} = \frac{\delta S}{S}\frac{f}{Q}, \tag{20}$$

where $S/\delta S$ is the signal-to-noise ratio and $Q = f/\gamma$ is the quality factor. For shot-noise-limited experiments, $\delta S/S = \sqrt{e/(I\tau)}$, where e is the magnitude of the electron charge, I is the average detector current, and τ is the integration time. For example, a shot-noise-limited experiment with $Q = 10^8$ (such as $\gamma = 3$ MHz, $f = 300$ THz) and $I = 1$ mA of average current would have a statistical limit of $\delta f/f \sim 1 \times 10^{-16}/\sqrt{\tau/\text{s}}$. Equation (16) converts this frequency limit to $\delta\mu/\mu$ by use of the relative sensitivity K_μ and the decaying response for $f_\phi \gtrsim \gamma$. For $f_\phi \ll \gamma$ and $K_\mu = -0.5$, the same example's shot-noise limit is $\delta\mu/\mu \sim 2 \times 10^{-16}/\sqrt{\tau/\text{s}}$. In a realistic experiment, laser technical noise may dominate over shot noise at low frequencies [44]. Because the molecules cannot effectively track oscillations with $f_\phi \gg \gamma$, the statistical sensitivity to μ at high frequencies becomes modulation-frequency-dependent. Keeping the same example, it is $\delta\mu/\mu \sim 8 \times 10^{-23}(f_\phi/\text{Hz})/\sqrt{\tau/\text{s}}$. Note that this fast-modulation result is actually independent of γ.

6. Conclusion

Molecular vibrations are leading systems for next-generation searches for drifts in μ and for the first-ever direct searches for oscillations in μ. The absolute sensitivity of vibrational frequencies to μ can be estimated with a relatively simple anharmonic oscillator model. Several molecules possess optical-frequency vibrational overtones with potential instabilities at the 10^{-18} level or below, comparable to the best atomic clocks. Experiments are underway with a variety of molecules, with most currently refining the state-control techniques. Future results will discover or further constrain the couplings and masses of new fields, with implications for quantum gravity and dark matter.

Acknowledgments

References

[1] Fritz Riehle, Patrick Gill, Felicitas Arias, and Lennart Robertsson. The CIPM list of recommended frequency standard values: guidelines and procedures. *Metrologia*, 55:188–200, 2018. doi: 10.1088/1681-7575/aaa302.

[2] Andrew D. Ludlow, Martin M. Boyd, Jun Ye, E. Peik, and P. O. Schmidt. Optical atomic clocks. *Rev. Mod. Phys.*, 87:637–701, 2015. doi: 10.1103/RevModPhys.87.637.

[3] M. S. Safronova, D. Budker, D. DeMille, Derek F. Jackson Kimball, A. Derevianko, and Charles W. Clark. Search for new physics with atoms and molecules. *Rev. Mod. Phys.*, 90:025008, 2018. doi: 10.1103/RevModPhys.90.025008.

[4] Jean-Philippe Uzan. Varying constants, gravitation and cosmology. *Living Rev. Relativity*, 14:2, 2011. doi: 10.12942/lrr-2011-2.

[5] Asimina Arvanitaki, Junwu Huang, and Ken Van Tilburg. Searching for dilaton dark matter with atomic clocks. *Phys. Rev. D*, 91:015015, Jan 2015. doi: 10.1103/PhysRevD.91.015015.

[6] Y. V. Stadnik and V. V. Flambaum. Can dark matter induce cosmological evolution of the fundamental constants of nature? *Phys. Rev. Lett.*, 115:201301, 2015. doi: 10.1103/PhysRevLett.115.201301.

[7] Aurélien Hees, Olivier Minazzoli, Etienne Savalle, Yevgeny V. Stadnik, and Peter Wolf. Violation of the equivalence principle from light scalar dark matter. *Phys. Rev. D*, 98:064051, 2018. doi: 10.1103/PhysRevD.98.064051.

[8] Riccardo Catena and Piero Ullio. A novel determination of the local dark matter density. *J. Cosmology Astroparticle Phys.*, 2010:004, 2010. doi: 10.1088/1475-7516/2010/08/004.

[9] Peter W. Graham, David E. Kaplan, and Surjeet Rajendran. Cosmological relaxation of the electroweak scale. *Phys. Rev. Lett.*, 115:221801, 2015. doi: 10.1103/PhysRevLett.115.221801.

[10] Abhishek Banerjee, Hyungjin Kim, and Gilad Perez. Coherent relaxion dark matter. *Phys. Rev. D*, 100:115026, 2019. doi: 10.1103/PhysRevD.100.115026.

[11] Y. V. Stadnik and V. V. Flambaum. Improved limits on interactions of low-mass spin-0 dark matter from atomic clock spectroscopy. *Phys. Rev. A*, 94:022111, 2016. doi: 10.1103/PhysRevA.94.022111.

[12] Nissim Kanekar. Constraining changes in the proton-electron mass ratio with inversion and rotation lines. *Astrophys. J. Lett.*, 728:L12, 2011. doi: 10.1088/2041-8205/728/1/L12.

[13] J. Bagdonaite, M. Daprà, P. Jansen, H. L. Bethlem, W. Ubachs, S. Muller, C. Henkel, and K. M. Menten. Robust constraint on a drifting proton-to-electron mass ratio at $z = 0.89$ from methanol observation at three radio telescopes. *Phys. Rev. Lett.*, 111:231101, 2013. doi: 10.1103/PhysRevLett.111.231101.

[14] W. Ubachs, J. Bagdonaite, E. J. Salumbides, M. T. Murphy, and L. Kaper. Colloquium: Search for a drifting proton-electron mass ratio from H_2. *Rev. Mod. Phys.*, 88:021003, 2016. doi: 10.1103/RevModPhys.88.021003.

[15] M. Daprà, P. Noterdaeme, M. Vonk, M. T. Murphy, and W. Ubachs. Analysis of carbon monoxide absorption at $z_{abs} \simeq 2.5$ to constrain variation of the proton-to-electron mass ratio. *MNRAS*, 467:3848–3855, 2017. doi: 10.1093/mnras/stx331.

[16] R. Lange, N. Huntemann, J. M. Rahm, C. Sanner, H. Shao, B. Lipphardt, Chr. Tamm, S. Weyers, and E. Peik. Improved limits for violations of local position invariance from atomic clock comparisons. 2020. arXiv:2010.06620.

[17] W. F. McGrew, X. Zhang, H. Leopardi, R. J. Fasano, D. Nicolodi, K. Beloy, J. Yao, J. A. Sherman, S. A. Schäffer, J. Savory, R. C. Brown, S. Römisch, C. W. Oates, T. E. Parker, T. M. Fortier, and A. D. Ludlow. Towards the optical second: Verifying optical clocks at the SI limit. *Optica*, 6:448–454, 2019. doi: 10.1364/OPTICA.6.000448.

[18] R. Schwarz, S. Dörscher, A. Al-Masoudi, E. Benkler, T. Legero, U. Sterr, S. Weyers, J. Rahm, B. Lipphardt, and C. Lisdat. Long term measurement of the ${}^{87}Sr$ clock frequency at the limit of primary Cs clocks. *Phys. Rev. Res.*, 2:033242, 2020. doi: 10.1103/PhysRevResearch.2.033242.

[19] V. V. Flambaum and A. F. Tedesco. Dependence of nuclear magnetic moments on quark masses and limits on temporal variation of fundamental constants from atomic clock experiments. *Phys. Rev. C*, 73:055501, 2006. doi: 10.1103/PhysRevC. 73.055501.

[20] J. Kobayashi, A. Ogino, and S. Inouye. Measurement of the variation of electron-to-proton mass ratio using ultracold molecules produced from laser-cooled atoms. *Nature Comm.*, 10:3771, 2019. doi: 10.1038/s41467-019-11761-1.

[21] A. Shelkovnikov, R. J. Butcher, C. Chardonnet, and A. Amy-Klein. Stability of the proton-to-electron mass ratio. *Phys. Rev. Lett.*, 100:150801, 2008. doi: 10.1103/PhysRevLett.100.15080.

[22] S. Schlamminger, K.-Y. Choi, T. A. Wagner, J. H. Gundlach, and E. G. Adelberger. Test of the equivalence principle using a rotating torsion balance. *Phys. Rev. Lett.*, 100:041101, 2008. doi: 10.1103/PhysRevLett.100.041101.

[23] Abhishek Banerjee, Dmitry Budker, Joshua Eby, Hyungjin Kim, and Gilad Perez. Relaxion stars and their detection via atomic physics. *Commun. Phys.*, 3:1, 2019. doi: 10.1038/s42005-019-0260-3.

[24] D. DeMille, S. Sainis, J. Sage, T. Bergeman, S. Kotochigova, and E. Tiesinga.

Enhanced sensitivity to variation of m_e/m_p in molecular spectra. *Phys. Rev. Lett.*, 100:043202, 2008. doi: 10.1103/PhysRevLett.100.043202.

[25] D. Hanneke, R. A. Carollo, and D. A. Lane. High sensitivity to variation in the proton-to-electron mass ratio in O_2^+. *Phys. Rev. A*, 94:050101(R), 2016. doi: 10.1103/PhysRevA.94.050101.

[26] Lawrence Krauss, John Moody, Frank Wilczek, and Donald E. Morris. Calculations for cosmic axion detection. *Phys. Rev. Lett.*, 55:1797–1800, 1985. doi: 10.1103/PhysRevLett.55.1797.

[27] Y. V. Stadnik and V. V. Flambaum. Searching for dark matter and variation of fundamental constants with laser and maser interferometry. *Phys. Rev. Lett.*, 114:161301, 2015. doi: 10.1103/PhysRevLett.114.161301.

[28] Andrei Derevianko. Detecting dark-matter waves with a network of precision-measurement tools. *Phys. Rev. A*, 97:042506, 2018. doi: 10.1103/PhysRevA.97.042506.

[29] C. L. Degen, F. Reinhard, and P. Cappellaro. Quantum sensing. *Rev. Mod. Phys.*, 89:035002, 2017. doi: 10.1103/RevModPhys.89.035002.

[30] Shlomi Kotler, Nitzan Akerman, Yinnon Glickman, and Roee Ozeri. Nonlinear single-spin spectrum analyzer. *Phys. Rev. Lett.*, 110:110503, 2013. doi: 10.1103/PhysRevLett.110.110503.

[31] Gerhard Herzberg. *Molecular Spectra and Molecular Structure, Vol. I: Spectra of Diatomic Molecules.* D. Van Nostrand Co., 1950. ISBN 0894642685.

[32] James K. G. Watson. The isotope dependence of diatomic Dunham coefficients. *J. Mol. Spec.*, 80:411–421, 1980. doi: 10.1016/0022-2852(80)90152-6.

[33] K. Beloy, M. G. Kozlov, A. Borschevsky, A. W. Hauser, V. V. Flambaum, and P. Schwerdtfeger. Rotational spectrum of the molecular ion NH^+ as a probe for α and m_e/m_p variation. *Phys. Rev. A*, 83:062514, 2011. doi: 10.1103/PhysRevA.83.062514.

[34] L. F. Pašteka, A. Borschevsky, V. V. Flambaum, and P. Schwerdtfeger. Search for the variation of fundamental constants: Strong enhancements in $X\,^2\Pi$ cations of dihalogens and hydrogen halides. *Phys. Rev. A*, 92:012103, 2015. doi: 10.1103/PhysRevA.92.012103.

[35] T. Zelevinsky, S. Kotochigova, and Jun Ye. Precision test of mass-ratio variations with lattice-confined ultracold molecules. *Phys. Rev. Lett.*, 100:043201, 2008. doi: 10.1103/PhysRevLett.100.043201.

[36] V. V. Flambaum and M. G. Kozlov. Enhanced sensitivity to the time variation of the fine-structure constant and m_p/m_e in diatomic molecules. *Phys. Rev. Lett.*, 99:150801, 2007. doi: 10.1103/PhysRevLett.99.150801.

[37] K. Beloy, A. Borschevsky, V. V. Flambaum, and P. Schwerdtfeger. Effect of α variation on a prospective experiment to detect variation of m_e/m_p in diatomic molecules. *Phys. Rev. A*, 84:042117, 2011. doi: 10.1103/PhysRevA.84.042117.

[38] Y. Song, M. Evans, C. Y. Ng, C.-W. Hsu, and G. K. Jarvis. Rotationally resolved pulsed field ionization photoelectron bands of $O_2^+(X\,^2\Pi_{1/2,3/2g}, v^+ = 0 - 38)$ in the energy range of $12.05 - 18.15$ eV. *J. Chem. Phys.*, 111:1905–1916, 1999. doi: 10.1063/1.479459.

[39] Ryan Carollo, Alexander Frenett, and David Hanneke. Two-photon vibrational transitions in $^{16}O_2^+$ as probes of variation of the proton-to-electron mass ratio. *Atoms*, 7:1, 2018. doi: 10.3390/atoms7010001.

[40] Colin J. Kennedy, Eric Oelker, John M. Robinson, Tobias Bothwell, Dhruv Kedar, William R. Milner, G. Edward Marti, Andrei Derevianko, and Jun Ye. Precision metrology meets cosmology: Improved constraints on ultralight dark matter from atom-cavity frequency comparisons. 2020. arXiv:2008.08773.

[41] Schlomi Kotler, Nitzan Akerman, Yinnon Glickman, Anna Keselman, and Roee Ozeri. Single-ion quantum lock-in amplifier. *Nature*, 473:61–65, 2011. doi: 10.1038/nature10010.

[42] Shahaf Aharony, Nitzan Akerman, Roee Ozeri, Gilad Perez, Inbar Savoray, and Ravid Shaniv. Constraining rapidly oscillating scalar dark matter using dynamic decoupling. 2019. arXiv:1902.02788.

[43] Wolfgang Demtröder. *Laser Spectroscopy.* Springer, 5 edition, 2014.

[44] D. Antypas, O. Tretiak, A. Garcon, R. Ozeri, G. Perez, and D. Budker. Scalar dark matter in the radio-frequency band: Atomic-spectroscopy search results. *Phys. Rev. Lett.*, 123:141102, 2019. doi: 10.1103/PhysRevLett.123.141102.

[45] Dionysios Antypas, Dmitry Budker, Victor V. Flambaum, Mikhail G. Kozlov, Gilad Perez, and Jun Ye. Fast apparent oscillations in fundamental constants. *Ann. Phys. (Berlin)*, 532:1900566, 2020. doi: 10.1002/andp.201900566.

[46] Xin Tong, Alexander H. Winney, and Stefan Willitsch. Sympathetic cooling of molecular ions in selected rotational and vibrational states produced by threshold photoionization. *Phys. Rev. Lett.*, 105:143001, 2010. doi: 10.1103/PhysRevLett. 105.143001.

[47] Patrick R. Stollenwerk, Mark G. Kokish, Antonio G. S. de Oliveira-Filho, Fernando R. Ornellas, and Brian C. Odom. Optical pumping of TeH^+: Implications for the search for varying m_p/m_e. *Atoms*, 6:53, 2018. doi: 10.3390/atoms6030053.

[48] Chin-wen Chou, Christoph Kurz, David B. Hume, Philipp N. Plessow, David R. Leibrandt, and Dietrich Leibfried. Preparation and coherent manipulation of pure quantum states of a single molecular ion. *Nature*, 545:203–207, 2017. doi: 10.1038/nature22338.

[49] S. S. Kondov, C.-H. Lee, K. H. Leung, C. Liedl, I. Majewska, R. Moszynski, and T. Zelevinsky. Molecular lattice clock with long vibrational coherence. *Nature Phys.*, 15:1118–1122, 2019. doi: 10.1038/s41567-019-0632-3.

[50] U. Bressel, A. Borodin, J. Shen, M. Hansen, I. Ernsting, and S. Schiller. Manipulation of individual hyperfine states in cold trapped molecular ions and

application to HD$^+$ frequency metrology. *Phys. Rev. Lett.*, 108:183003, 2012. doi: 10.1103/PhysRevLett.108.183003.

[51] P. O. Schmidt, T. Rosenband, C. Langer, W. M. Itano, J. C. Bergquist, and D. J. Wineland. Spectroscopy using quantum logic. *Science*, 309:749–752, 2005. doi: 10.1126/science.1114375.

[52] Andrew A. Geraci, Colin Bradley, Dongfeng Gao, Jonathan Weinstein, and Andrei Derevianko. Searching for ultralight dark matter with optical cavities. *Phys. Rev. Lett.*, 123:031304, 2019. doi: 10.1103/PhysRevLett.123.031304.

[53] Matthias Germann, Xin Tong, and Stefan Willitsch. Observation of electric-dipole-forbidden infrared transitions in cold molecular ions. *Nature Phys.*, 10:820–824, 2014. doi: 10.1038/NPHYS3085.

[54] Mudit Sinhal, Ziv Meir, Kaveh Najafian, Gregor Hegi, and Stefan Willitsch. Quantum-nondemolition state detection and spectrocsopy of single trapped molecules. *Science*, 367:1213–1218, 2020. doi: 10.1126/science.aaz9837.

[55] Fabian Wolf, Jan C. Heip, Maximilian J. Zawierucha, Chunyan Shi, Silke Ospelkaus, and Piet O. Schmidt. Prospect for precision quantum logic spectroscopy of vibrational overtone transitions in molecular oxygen ions. 2020. arXiv:2002.05584.

[56] Masatoshi Kajita. Accuracy estimation for the $^{16}O_2^+$ transition frequencies targeting the search for the variation in the proton-electron mass ratio. *Phys. Rev. A*, 95: 023418, 2017. doi: 10.1103/PhysRevA.95.023418.

[57] J. Biesheuvel, J.-Ph. Karr, L. Hilico, K. S. E. Eikema, W. Ubachs, and J. C. J. Koelemeij. Probing QED and fundamental constants through laser spectroscopy of vibrational transitions in HD$^+$. *Nature Comms.*, 7:10385, 2016. doi: 10.1038/ncomms10385.

[58] S. Alighanbari, G. S. Giri, F. L. Constantin, V. I. Korobov, and S. Schiller. Precise test of quantum electrodynamics and determination of fundamental constants with HD$^+$ ions. *Nature*, 581:152–158, 2020. doi: 10.1038/s41586-020-2261-5.

[59] Sayan Patra, M. Germann, J.-Ph. Karr, M. Haidar, L. Hilico, V. I. Korobov, F. M. J. Cozijn, K. S. E. Eikema, W. Ubachs, and J. C. J. Koelemeij. Proton-electron mass ratio from laser spectroscopy of HD$^+$ at the part-per-trillion level. *Science*, 2020. doi: 10.1126/science.aba0453.

[60] S. Schiller and V. Korobov. Tests of time independence of the electron and nuclear masses with ultracold molecules. *Phys. Rev. A*, 71:032505, 2005. doi: 10.1103/PhysRevA.71.032505.

[61] S. Schiller, D. Bakalov, and V. I. Korobov. Simplest molecules as candidates for precise optical clocks. *Phys. Rev. Lett.*, 113:023004, 2014. doi: 10.1103/PhysRevLett.113.023004.

[62] Mark G. Kokish, Patrick R. Stollenwerk, Masatoshi Kajita, and Brian C. Odom. Prospects for polar-molecular-ion optical probe of varying proton-electron mass ratio. *Phys. Rev. A*, 98:052513, 2018. doi: 10.1103/PhysRevA.98.052513.

[63] Lincoln D. Carr, David DeMille, Roman V. Krems, and Jun Ye. Cold and ultracold molecules: science, technology, and applications. *New J. Phys.*, 11:055049, 2009. doi: 10.1088/1367-2630/11/5/055049.

[64] John Brown and Alan Carrington. *Rotational Spectroscopy of Diatomic Molecules.* Cambridge University Press, 2003.

[65] S. M. Brewer, J.-S. Chen, A. M. Hankin, E. R. Clements, C. W. Chou, D. J. Wineland, D. B. Hume, and D. R. Leibrandt. ^{27}Al$^+$ quantum-logic clock with a systematic uncertainty below 10^{-18}. *Phys. Rev. Lett.*, 123:033201, 2019. doi: 10.1103/PhysRevLett.123.033201.

[66] Masatoshi Kajita, Geetha Gopakumar, Minori Abe, Masahiko Hada, and Matthias Keller. Test of m_p/m_e changes using vibrational transitions in N$_2^+$. *Phys. Rev. A*, 89:032509, 2014. doi: 10.1103/PhysRevA.89.032509.

[67] W. M. Itano, J. C. Bergquist, J. J. Bollinger, J. M. Gilligan, D. J. Heinzen, F. L. Moore, M. G. Raizen, and D. J. Wineland. Quantum projection noise: Population fluctuations in two-level systems. *Phys. Rev. A*, 47:3554–3570, 1993. doi: 10.1103/PhysRevA.47.3554.